ÉCOLE POLYTECHNIQUE FÉDÉRALE DE LAUSANNE

Fabry-Perot Interferometer

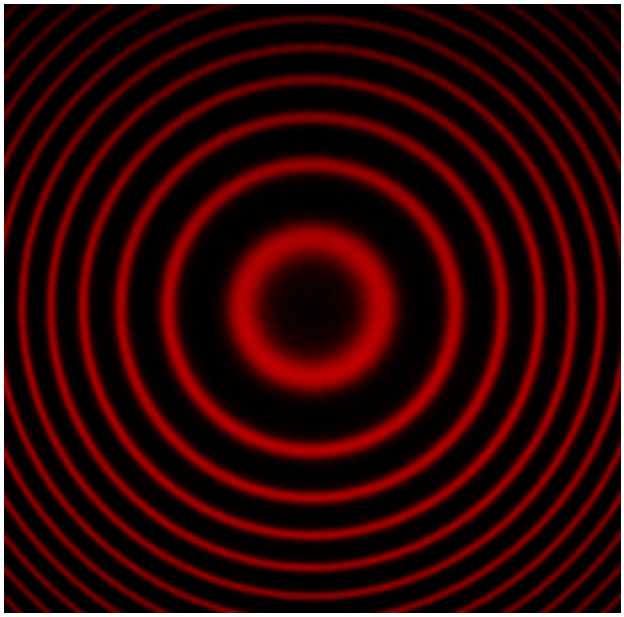

Tanguy Falkenback (†), Ambrine Douhane (§)
Sciper : [350603] (†), [282708] (§)
Course : MICRO - 423
Teachers : Ye Pu & Demetri Psaltis
TA : Tao Jiang
Date : March 11, 2026

EPFL

CONTENTS

LIST OF FIGURES

LIST OF TABLES

***Abstract*—This report summarizes the experimental results obtained to gain theoretical understanding and practical knowledge of Fabry-Perot Interferometer. Different configurations are studied (confocal, concentric, ...) and with various lenses. With a ROC (radius of curvature) of 75 mm, the experimental finesse is $F_R = 32.08$, the free spectral range is $\delta v = 881.74\ MHz$ and the spectral resolution is $\Delta v = 27.49\ MHz$. With a ROC of 100 mm, the experimental finesse is $F_R = 14.36$, the free spectral range is $\delta v = 651.72\ MHz$ and the spectral resolution is $\Delta v = 45.38\ MHz$.**

I. Introduction

Interferometry is a method commonly used in many fields of science (astronomy, metrology, oceanography, seismology...) to extract information from the interference of some waves. The Michelson interferometer and the Mach-Zenhder one are two of the more famous interferometers (see Figures 1 and 2) and are based on amplitude splitting.

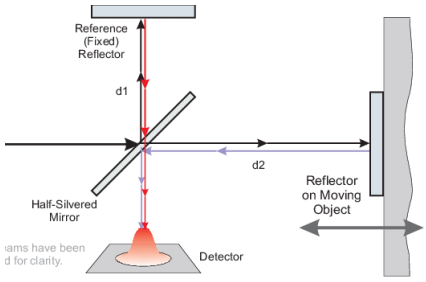

Fig. 1. Schematic representation of Michelson interferometer [10]

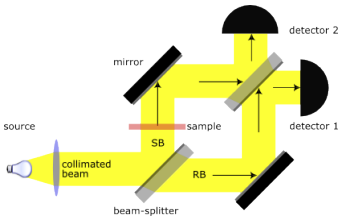

Fig. 2. Schematic representation of Mach-Zenhder interferometer [11]

This laboratory will focus on Fabry-Perot interferometer. It is typically an optical cavity formed by two parallel and closely spaced thin mirrors of reflective surfaces, that let some optical waves pass through the optical cavity if and only if they are in resonance with it. In fact, each time the light reaches the second mirror a small proportion of of the light is transmitted through it, which induces multiple offset beams that can interfere with each others. The large number of interfering rays produces an interferometer with very high resolution.

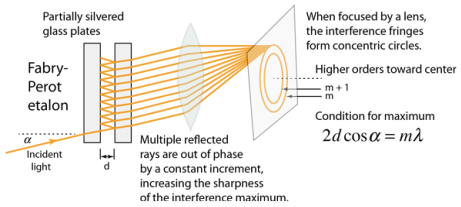

Fig. 3. Schematic representation of Fabry-Perot interferometer [12]

II. Theoretical background

The purpose of this chapter is to answer the questions asked in the assignment in order to develop the theory of optical fibers. Most of the answers can be found in the assignment theory chapter [1].

- Find an energy diagram with the different atoms levels for the He Ne laser. You can explain the operation principle of a HeNe laser ?

A helium–neon laser (or He-Ne laser) is composed of a mixture of helium and neon gases with ratio of usually 10:1 or 5:1. The creation of the laser beams happens when the inversion of population occurs, i.e. when the numbers Ni of electrons in the higher energy states E_i are bigger than the N_0, the number of electrons in lower energy state E_0. To do this, one shall pump the mean. This is done by placing two electrodes in the cavity: one cathode and one anode. Then, some high DC voltage is applied which creates an electric field that ionizes the gas. Since the energy of the excited states of helium atoms is very similar to neon's ones, the energy of helium is transferred to neon by successive collisions, which bring thus helium atoms to ground state and neon atoms in higher metastable E3 and E5 energy states. After a while, spontaneous emission happens: the latters spontaneously fall down into the next lower energy states (E2 and E4) by yielding some optical energy. This energy is basically photons with a certain wavelength, in particular $\lambda = 632.8\,\mathrm{nm}$ (see Figure 4).

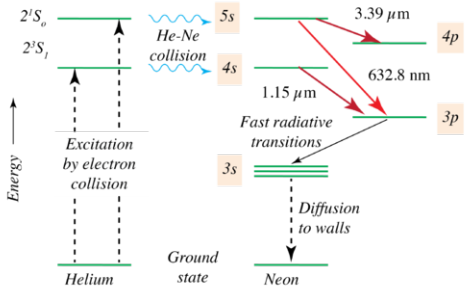

Fig. 4. Energy levels in a He-Ne Laser [2]

- What are the modes in a resonator (cavity) ?

The modes in a resonators are defined as some particular shape of the propagating field such that their phase shift induced by a round-trip in the cavity is equal to a multiple of 2π [13].

Two types of modes exist: transversal and longitudinal. Tranversal modes occur because of boundary conditions imposed by the waveguide, when the electric field is perpendicular to its direction of propagation. Longitudinal modes are the result of wavelengths for which the light beam in the cavity forms a standing wave, while it is interfering.

- What determines the number of modes in a resonator (cavity) ?

The number of modes m in a cavity is a strictly positive integer, and depends on its length L in meters, the wavelength of the electromagnetic field λ in meters and the index of refraction of the propagation mean n: $m = \frac{2nL}{\lambda}$.

$$m = \frac{2L_c}{\lambda_m} = \frac{2nL}{\lambda_0} \geq 1 \tag{1}$$

To go from the left term to the right term in Equation (1), the relation $\lambda_m = \frac{\lambda_0}{n}$ is used.

- How does a piezo actuator works ?

Piezoelectricity is a property through which a mechanical stress generates charges. This is used in piezo actuators: one applies some electric field in the material, which turns into mechanical strain which implies bending. Typical piezoelectric materials used for actuation are ZnO, Quartz, AlN or PZT [4].

- What is the temporal coherence length and how is it measured ?

The temporal coherence length L_c is equal to the difference d of optical paths on which the fringes visibility on a Michelson interferogram is greater or equal to half the maximum visibility at $d = 0\,\mathrm{m}$. It is given by the formula of Equation (2).

$$L_c = \frac{c}{n\nu} \tag{2}$$

Where $c = 3.00 \times 10^8\,\mathrm{ms}^{-1}$ is the celerity of the light, n the refractive index of the medium, and ν is the frequency of the light in Hz. For a HeNe laser, depending on whether the laser is single or multi mode, this length varies between few tens of centimeters to few tens of meters, depending on whether the laser is single or multimode.

- Find a sensitivity curve of a silicon photo diode. Can you explain why there is a cut-off wavelength ?

Figure 5 shows the variation of the absolute responsivity for different wavelengths. The absolute responsivity of a photodiode is the ratio between the input and the output of a system. It is a measurement of gain. Based on the graph, it is visible that the maximum occurs for a wavelength around $0.9\,\mu\mathrm{m}$. Before this λ, the curve slowly increases and after $0.9\,\mu\mathrm{m}$, the curve strongly decreases. This fall is due to the too small energy given by the photon. As a reminder, the energy of the incoming photon has to be greater than the bandgap energy and the energy of a photon is inversely proportional to the wavelength according to Equation (3).

$$E_{photon} = h\nu = \frac{hc}{\lambda} \tag{3}$$

Where h is Boltzmann's constant ($= 6.63 \times 10^{34}\ Js$), ν is the frequency, c is the speed of light ($= 3 \times 10^8\ m/s$) and λ is the wavelength. The slow decrease for high frequencies is due to the thermal losses because of the surplus of energy but this behaviour is slower.

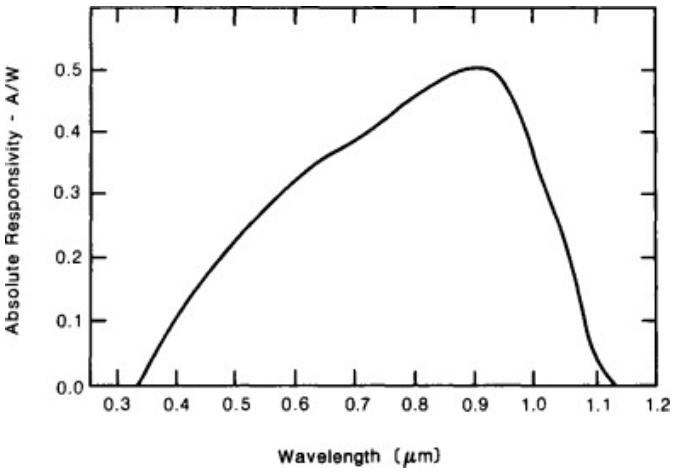

Fig. 5. Variation of the absolute responsivity with the wavelength

- What is the design principle of a dichroic filter ? Why one uses dichroic filters in multiple interference setups ?

A dichroic filter is a filter which properties depend on wavelengths. Depending on its coating, it will allow, or not, the incoming light to be transmitted. To obtain the result in the wanted range, it is interesting to use dichroic filters and thus avoid studying the whole spectrum. Interference of all the wavelength would be chaotic to analyze.

III. Experiment 1 - Measurements of confocal setup with $ROC = 75\,\mathrm{mm}$ for spherical mirrors

This experiment aims to identify the parameters finesse, FSR and FWHM of a cavity with confocal configuration for $ROC = 75\,\mathrm{mm}$. To do this, several measures are performed using the oscilloscope based on the signal received by the CMOS camera.

A. Setup

The setup used in shown in Figure 6. It composed by a HeNe laser that emits light, which goes into a beam expander before reaching the cavity. One mirror is fixed, and the other one can have its position modified by a piezo-driver to make the distance between the mirrors change, and so the modes of the cavity. Then, the ray is focused and capted by a photo diode plugged to the oscilloscope. All the tools are fixed on a optical ray to avoid security issues, but also to make their alignment more convenient.

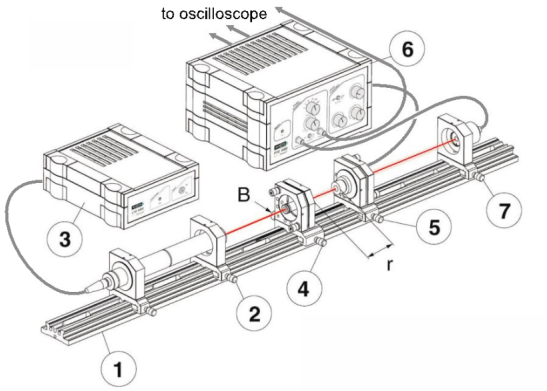

Fig. 6. Setup for the first experiment with (1) optical rail – (2) laser with mounting – (3) laser power supply – (4) fixed resonator mirror – (5) piezo-driven resonator mirror – (6) control unit – (7) photo diode [1] [18]

B. Experimental results

The first step of this experiment is to compute the finesse F_R. This measurement characterize the performance of the resonator and is taken for well aligned mirrors. The finesse is experimentally limited to 50 due to the nature of the reflective surface even for high precision mirrors. The finesse is found according to Equation (4) [5].

$$F_R = \frac{\delta\tau}{\Delta\tau} \tag{4}$$

Where $\delta\tau$ is the time between two peaks and $\Delta\tau$ is the width of a peak.

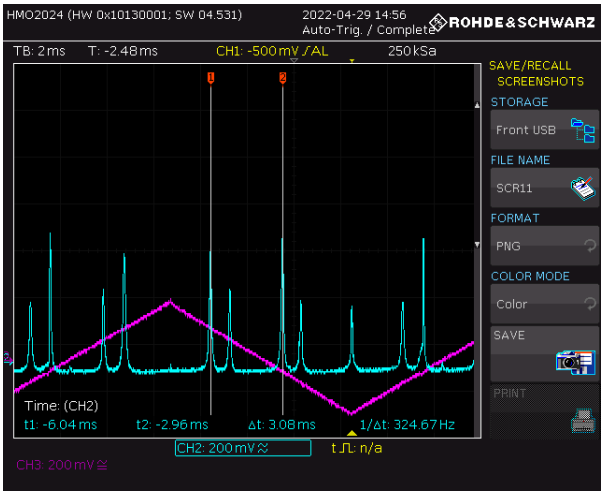

Fig. 7. Output of the oscilloscope to visualize the distance between two peaks.

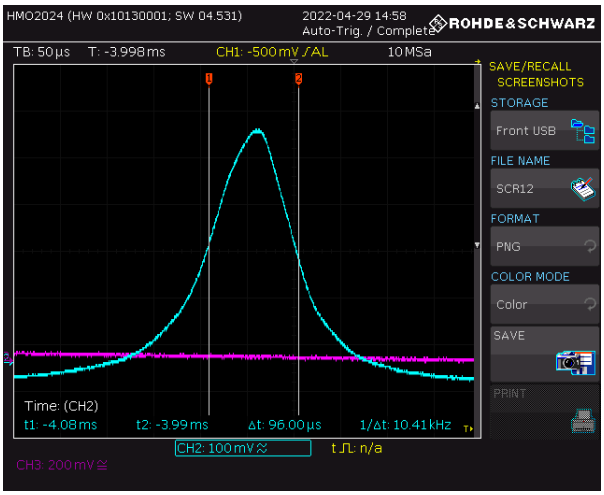

Fig. 8. Output of the oscilloscope to visualize the width of a peak.

Based on Figures 7 and 8, the two values are found. $\delta\tau = 3.08\ ms$ and $\Delta\tau = 96\ \mu m$ giving a finesse $F_R = 32.08$. To compute the plausible error done, an error of 2% is taken for both measurements. This implies the following statements: $\delta\tau = 3.08 \pm 0.06\ ms$ and $\Delta\tau = 96 \pm 1.92\ \mu m$. The range for the error committed on F_R is then given by Equations (6) and (5 where the extreme cases are considered.

$$F_{min} = \frac{3.08 - 0.06\ ms}{96 + 1.92\ \mu m} = 30.83 \tag{5}$$

$$F_{max} = \frac{3.08 + 0.06\ ms}{96 - 1.92\ \mu m} = 33.39 \tag{6}$$

The next parameter to compute is the FSR (free spectral range). According to the lab notes, the formula for the FSR is given by Equation (41) because the case analyzed is using plane mirrors [1].

$$\delta\nu = \frac{c}{4d} \tag{7}$$

Where c is the speed of light and d is the distance between the two mirrors so it represents the size of the cavity. The value of d for this first experiment is $d = 8.5\ cm$ and the exact constant for the speed of light is $c = 299792458\ m/s$ [3]. This allow to compute the free spectral range : $\delta\nu = 881.74\ MHz$. Once again, an error of 2% on the measurement of the distance will be considered. The interval of error for the free spectral range is found here under.

$$\delta\nu_{min} = \frac{299792458\ m/s}{4 \times (8.5 + 0.17\ cm)} = 864.45\ MHz \tag{8}$$

$$\delta\nu_{max} = \frac{299792458\ m/s}{4 \times (8.5 - 0.17\ cm)} = 899.74\ MHz \tag{9}$$

The last parameter to compute is the spectral resolution. This value is simply found using the finesse formula from the lab notes [1] described in Equation (10).

$$F = \frac{\delta\nu}{\Delta\nu} \iff \Delta\nu = \frac{\delta\nu}{F} = 27.49\ MHz \tag{10}$$

As previously done, it is possible to obtain a range of error for the spectral resolution using the two previous range. This gives equations (11) and (12).

$$\Delta\nu_{min} = \frac{\delta\nu_{min}}{F_{max}} = 25.89\ MHz \tag{11}$$

$$\Delta\nu_{max} = \frac{\delta\nu_{max}}{F_{min}} = 29.18\ MHz \tag{12}$$

C. Theoretical results

The theoretical value for the finesse is defined by the coefficient of reflection of the mirror. In the case of this laboratory, $R = 0.96$ because $T = 4\%$ (see sticker on mirror) and $R + T = 1$.

$$F_R = \pi\frac{\sqrt{R}}{1 - R} = 76.95 \tag{13}$$

This value is larger than the one measured but as explained before, the real value can't exceed 50 due to mirrors properties.

For the computation of the FSR, the value of d is the theoretical value between the two mirrors defined by the ROC of the mirror because of the confocal configuration [1]. In this first experiment, $ROC = d = 75\ mm$. Therfore, the value of $\delta\nu$ is set to $999.3\ MHz$ using Equation (41).

The last variable is determine based on the two previous ones using equation (10). This gives $\Delta\nu = 12.99\ MHz$. This value is half the one measured due to the big variation in the finesse parameter.

Table I sums up the values obtained for this first experiment.

TABLE I
COMPARISON BETWEEN THE THEORETICAL AND EXPERIMENTAL VALUES

Variable	Theoretical	Experimental	Units
F	76.95	32.08	-
$\delta\nu$	999.3	881.74	MHz
$\Delta\nu$	12.99	27.49	MHz

It is now possible to assess the error percentage of each variable. This is computed as followed:

$$\text{error} = \frac{|\text{theoretical} - \text{experimental}|}{\text{theoretical}} \tag{14}$$

TABLE II
ERROR PERCENTAGES FOR THE 3 VARIABLES

Variable	|Difference|	Units	Error
F	44.87	-	58.31%
$\delta\nu$	117.56	MHz	11.76%
$\Delta\nu$	14.5	MHz	111.62%

D. Wavelength separation

To obtain the wavelength separation, The phase shift between two twins must be computed. This is done by performing a ratio of the time between two twins and the time between two peaks (not twins).

$$\Delta\phi = \pi\frac{\delta\tau_{twins}}{\delta\tau} \tag{15}$$

The value of $\delta\tau$ is already known and shown on Figure 7. The value of $\delta\tau_{twins}$ is visible on Figure 9 and equal to $778\ \mu m$. By putting the values of the variables in Equation (15), the phase difference is equal to 0.79 radians.

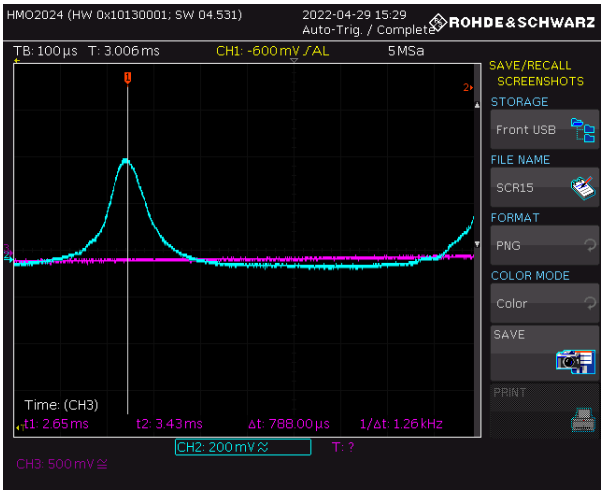

Fig. 9. Time separation between two twins

To link the wavelength separation with the phase difference, the expression of the phase is useful. As a reminder, a phase can be expressed as follows:

$$\phi = knd' = \frac{4\pi nd}{\lambda} \tag{16}$$

Where k is the wavelength number, n is the index of refraction in the air and d' is the distance travelled by the wave. By substituting the definition of $k = \frac{2\pi}{\lambda}$ and the distance travelled $d' = 2d$ (going back and forth) the second term is obtained. The expression of the phase difference is written in Equation (17).

$$\Delta\phi = k_1 nd' - k_2 nd' = \frac{4\pi nd}{\lambda_1} - \frac{4\pi nd}{\lambda_2} = \frac{4\pi nd\Delta\lambda}{\lambda^2} \tag{17}$$

The denominator of Equation (17)'s expression is λ^2 because it is assumed than λ_1 and λ_2 are very close. Nevertheless, the difference is not negligible (not 0). By reversing last equation in order to isolate $\Delta\lambda$, Equation (18) is found.

$$\Delta\lambda = \frac{\Delta\phi\lambda^2}{4\pi nd} = 0.298\ pm \tag{18}$$

Plugging the values of the variables ($\lambda = 632.8\ nm$, $n = 1$ and $d = 8.5\ cm$) this gives a wavelength separation of $0.298\ pm$.

E. Polarization

The polarization is briefly studied in this laboratory. The three following plots (Figures 10,11 and 12) show that when a polarized lens is placed in front of the laser and that the angle is changed the outputs are not the same.

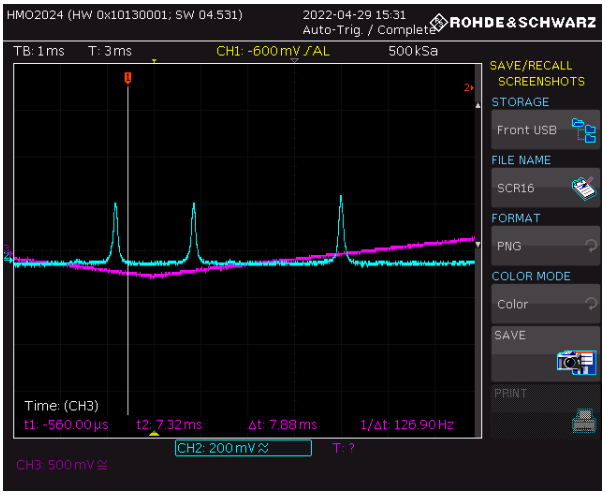

Fig. 10. Visualisation of the left twin (polarization = 64°)

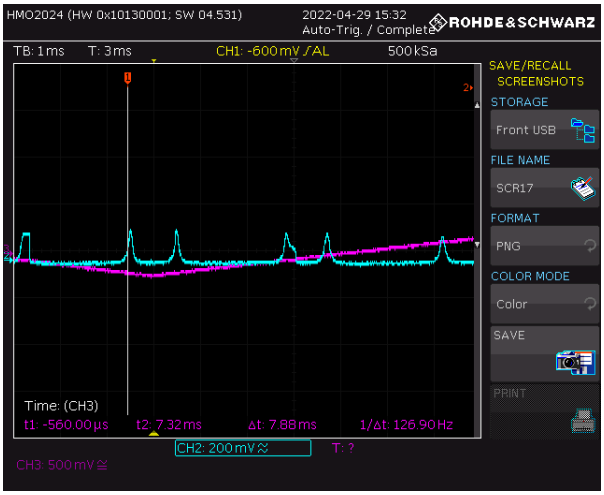

Fig. 11. Visualisation of both twins with equal amplitude (polarization = 94°)

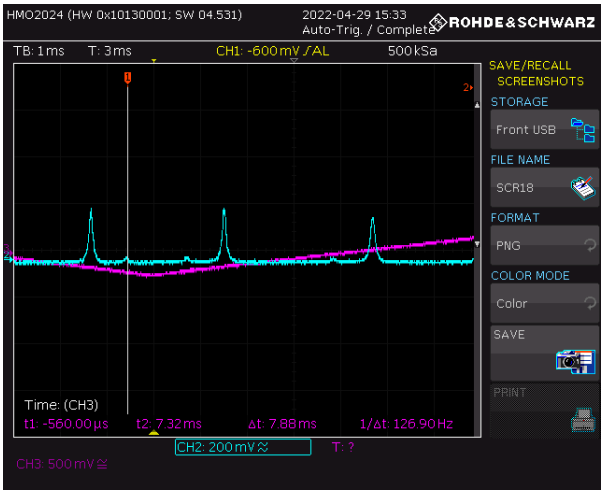

Fig. 12. Visualisation of the right twin (polarization = 129°)

When the angle is 64° as in Figure 10, one of the two twins is visible and the other one is completely blocked by the polarized lens. The same observation is possible for Figure 12 but this time for the other twin and for an angle of 129°. A case in between these two angles is also plotted to observe the behaviour during the transition (see Figure 11).

F. Piezo expansion rate

In order to compute the expansion rate of the piezo actuator, the slope of the triangular wave must be computed. The following development is performed for an increasing ramp but can also be done for a decreasing one. As a reminder, the equation of a line is $y = mx + p$ where m is the slope. This slope is computed according to Equation (19). Note that as the expansion is studied, the reference point p is not used.

$$m = \frac{\Delta y}{\Delta x} = \frac{550\ mV}{9.5\ ms} = 57.9\ V/s \tag{19}$$

The values for the x and y variation are found in Figures 13 and 14.

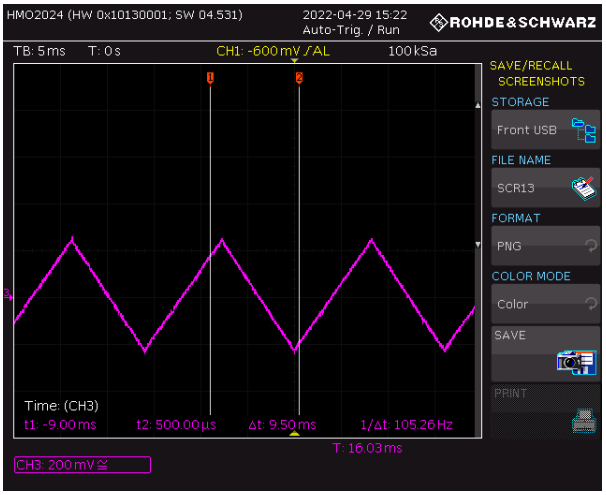

Fig. 13. Measurement of the time variation of the piezo

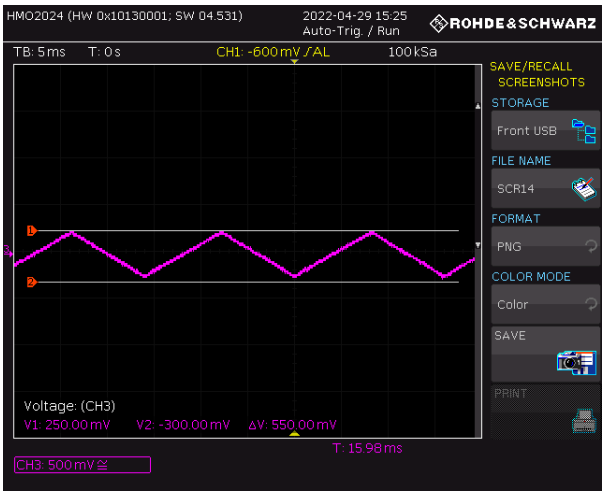

Fig. 14. Measurement of the voltage variation of the piezo

This expression is given in term of time but the piezo expansion is more interesting when it is expressed in term of the distance between the two mirrors (dimension of the cavity). Therefore, it is needed to retake the expression of the phase described in Equation (16). By reversing this equation the distance can be isolated (it is considered that a change of $\Delta\phi$ is responsible for a change of Δd).

$$\Delta d = \frac{\Delta\phi\lambda}{4\pi n} \tag{20}$$

The phase shift of the piezo is simply equal to the ratio between the time of a rising edge and the time of a period. Because of the periodicity of the signal used, the $\Delta\phi$ is equal to 2π (with $T_{piezo} = 9.5\ ms$).

$$\Delta\phi = \pi\frac{T_{piezo}}{\delta\tau_{piezo}} = 2\pi \tag{21}$$

Based on this observation, the Equation (20) becomes $\Delta d = \frac{\lambda}{2n}$ which is equal to $316.4\ nm$. The expansion rate in terms of the distance is then simply found using Equation (22).

$$R = \frac{\Delta d}{mT_{piezo}} = 575.22\ nm/V \tag{22}$$

IV. Experiment 2 - Measurements of confocal setup with $ROC = 100\,\text{mm}$ for spherical mirrors

Here also, this experiment aims to identify the parameters finesse, FSR and FWHM of a cavity with confocal configuration for $ROC = 100\,\text{mm}$. The value of d for this second experiment is $d = 11.5\ cm$.

A. Setup

The setup is exactly the same as the previous experiment except that the mirrors are changed to go from a ROC of $75\ mm$ to a ROC of $100\ mm$. Figure 6 can therefore be taken as a reference.

B. Results

The experiment beings the same as the previous one, the formulas for the finesse, the free spectral range and the spectral resolution are exactly the same as Equations (4), (41) and (10).

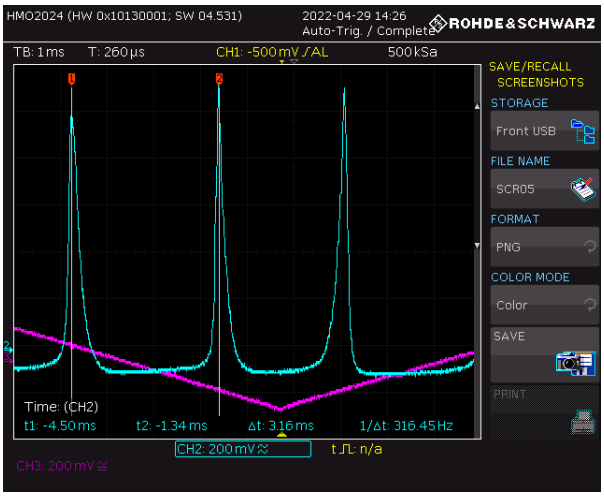

Fig. 15. Output of the oscilloscope to visualize the distance between two peaks.

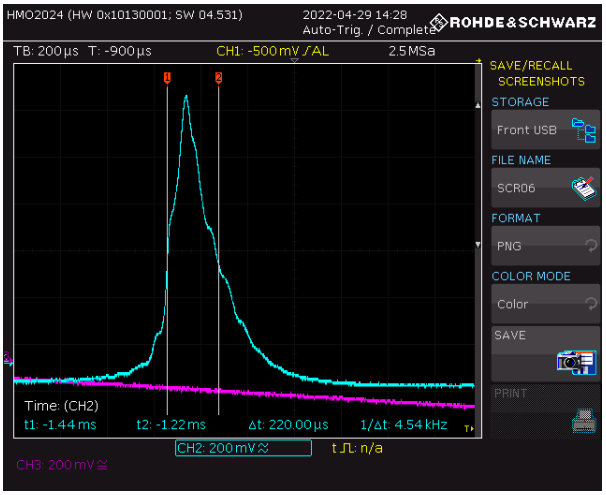

Fig. 16. Output of the oscilloscope to visualize the width of a peak.

For clarity, the formulas are written once more and the new values found on Figures 15 and 16 are plugged in ($\delta\tau = 3.16\ ms$ and $\Delta\tau = 220\ \mu m$). This gives Equation (23) for the finesse.

$$F_R = \frac{\delta\tau}{\Delta\tau} = \frac{3.16\ ms}{220\ \mu m} = 14.36 \tag{23}$$

By still considering an error of 2%, a range is created going from F_{min} to F_{max}.

$$F_{min} = \frac{3.16 - 0.0632\ ms}{220 + 4.4\ \mu m} = 13.8 \tag{24}$$

$$F_{max} = \frac{3.16 + 0.0632\ ms}{220 - 4.4\ \mu m} = 14.95 \tag{25}$$

Concerning the free spectral range (FSR), the Equations to reuse are (41), (8) and (9). In this problem the value of d is equal to $11.5\ cm$ giving the result and interval here under.

$$\delta\nu = \frac{c}{2d} = \frac{299792458\ m/s}{4 \times 11.5\ cm} = 651.72\ MHz \tag{26}$$

$$\delta\nu_{min} = \frac{299792458\ m/s}{4 \times (11.5 + 0.23\ cm)} = 638.94\ MHz \tag{27}$$

$$\delta\nu_{max} = \frac{299792458\ m/s}{4 \times (11.5 - 0.23\ cm)} = 665.02\ MHz \tag{28}$$

The spectral resolution can also be computed based on previous equations. The variables are set to their values for this case. The result and range are described in Equations (29), (30) and (31).

$$\Delta\nu = \frac{\delta\nu}{F} = 45.38\ MHz \tag{29}$$

$$\Delta\nu_{min} = \frac{\delta\nu_{min}}{F_{max}} = 44.49\ MHz \tag{30}$$

$$\Delta\nu_{max} = \frac{\delta\nu_{max}}{F_{min}} = 46.31\ MHz \tag{31}$$

C. Stability

In this subsection, one will mark the corresponding points for the confocal and the concentric cases. Then the stability criterion will be computed for all other combinations of mirrors used in this lab. The graph shown in Figure 17 is a stability plot. On it, have been drawn some points, corresponding to the results shown in tables III, IV and V. It is possible to state if the beam introduced in the cavity of dimensions r_1, r_2, and d will grow limitless until being lost in the cavity, or if the system is stable. The area under the curve is the stable zone (grey zone), which means, the points that solve Inequation (32) describe a stable configuration.

$$0 \leq (1 - \frac{d}{r_1})(1 - \frac{d}{r_2}) \leq 1 \tag{32}$$

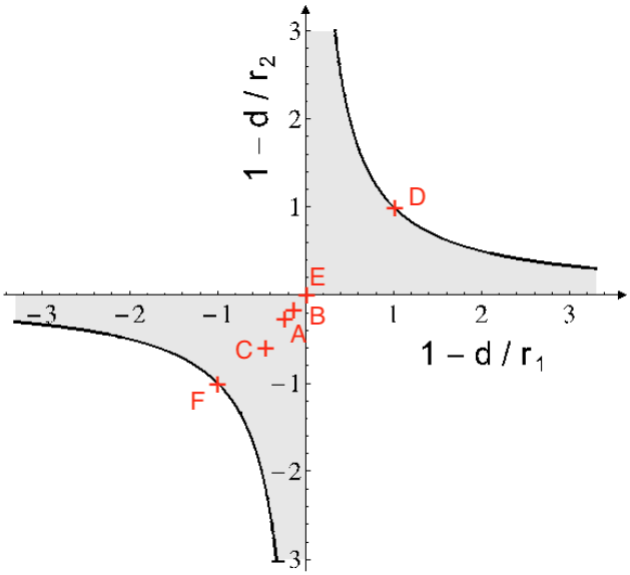

Fig. 17. Stability of optical resonators made of two mirrors with radii of curvature r1 and r2, separated by a distance d. The stable regions are gray shaded areas and include the central point. [1]
Practical points: A(-0.15;-0.15) symm. confocal $ROC = 100\,\mathrm{mm}$, B(-0.13;-0.13) symm. confocal $ROC = 75\,\mathrm{mm}$, C(-0.53;-0.53) symm. concentric
Theoretical points: D(1;1) planar, E(0;0) symm. confocal, F(-1;-1) symm. concentric

It is interesting to compute each stability criterion for all the configurations of cavities. In this study, we will use the one described in *Fundamentals of photonics* [19], they are shown in Table III.

TABLE III
ALL CAVITY CONFIGURATIONS [19]

Configuration	Expression
Confocal	$r_1 + r_2 = 2d$
Concentric	$r_1 + r_2 = d$
Symmetric confocal	$r_1 = r_2 = d$
Symmetric concentric	$r_1 = r_2 = 1/2d$
Semiconfocal	$r_1 = 2d,\ r_2 = \infty$
Plane	$r_1 = r_2 = \infty$

TABLE IV
THEORETICAL RESULTS FOR STABILITY FOR DIFFERENT CONFIGURATIONS

Configuration	r_1	r_2	d	$(1 - \frac{d}{r_1})(1 - \frac{d}{r_2})$
Confocal	$2d - r_2$	r_2	d	$(1 - \frac{d}{2d-r_2})(1 - \frac{d}{r_2})$
Concentric	$d - r_2$	r_2	d	$(1 - \frac{d}{d-r_2})(1 - \frac{d}{r_2})$
Symm. confocal	d	d	d	0
Symm. concentric	$\frac{d}{2}$	$\frac{d}{2}$	d	1
Plane	∞	∞	d	1

Note that d does not perfectly match with the theory in Table V, regarding its dependence to r_1 and r_2. d has been set such as, during the lab, high and well spaced peaks were observable on the oscilloscope.

TABLE V
PRACTICAL RESULTS FOR STABILITY FOR DIFFERENT CONFIGURATIONS - r_1, r_2 AND d IN MILLIMETERS

Configuration	r_1	r_2	d	$(1 - \frac{d}{r_1})(1 - \frac{d}{r_2})$
Symm. confocal	100	100	115	2.25×10^{-2}
Symm. confocal	75	75	85	1.78×10^{-2}
Symm. concentric	75	75	115	2.84×10^{-1}

Each case has its own point drawn in Figure 17 as a summary. It seams that the results obtained with the experiments are close to the theoretical ones. Also note that all points are in the grey area which means, all configurations are stable.

V. EXPERIMENT 3 - CHARACTERIZATION OF CONCENTRIC SETUP FOR PLANE-MIRROR CAVITY

Now for this new experiment, the idea is to create a planar cavity.

A. Setup

The setup of this experiment is shown in Figure 18. The use of a rail allows a good alignment of the optical objects. The light generated by the laser crosses the beam expander before being focused by a lens and reaching the cavity formed by two plane mirrors, one of these is piezo driven. Finally the light is again focused by a lens if needed, and the incoming light hits a CMOS camera which is connected to our software shown in Section VIII-A7. The software can help for alignment since it gives a real time image of the incoming light.

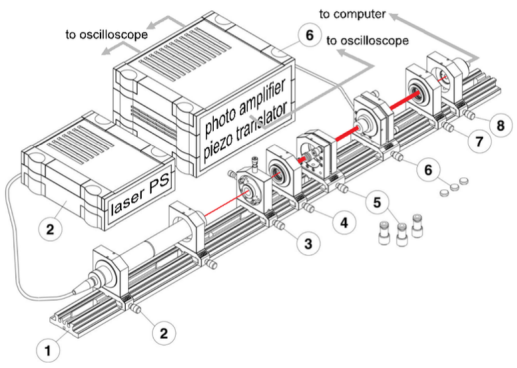

Fig. 18. Setup of the Fabry-Pérot resonator with plane mirrors: (1) optical rail – (2) laser with mounting and power supply – (3)+(4) beam expander – (5) fixed mirror – (6) piezo-driven mirror and control unit – (7) focusing lens – (8) CMOS camera. [18] [1].

B. Results

First, one can calculate the distance between the mirrors d and its standard deviation using the concentric ring system. If we plot the ring diameter on the ring number, one can obtain the graph of Figure 20 and extract some data from this.

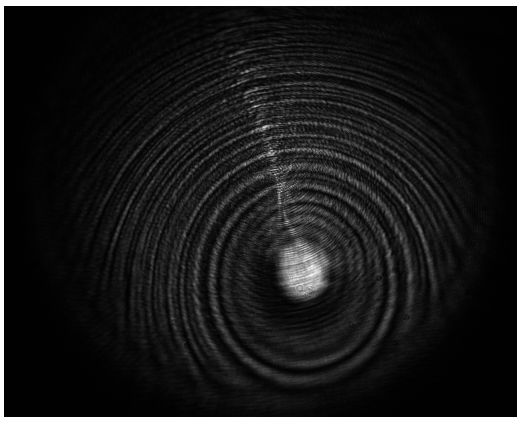

Fig. 19. Interference rings for $d = 12cm$

On Figure 20, we have the intensity of the light of Figure 19, depending on the pixel position in the horizontal direction.

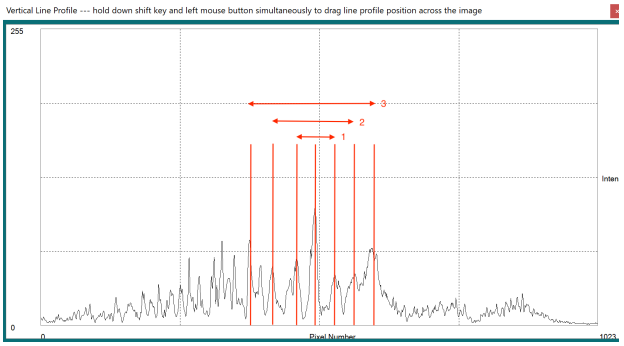

Fig. 20. Intensity of the interference rings for one central line

To get the diameters of the rings, we analyse this plot, were we just defined some peaks around the main one, and drew some arrows to see the rings well. The data sheet gives a ratio of $5.2\,\mu\text{m}$ by pixel [6]. We obtain: $d_1 = 71\text{pix} = 383\,\mu\text{m}$, $d_2 = 151\text{pix} = 815\,\mu\text{m}$, $d_3 = 227\text{pix} = 1226\,\mu\text{m}$. With Matlab, we get Figure 21. A linear regression is made in addition.

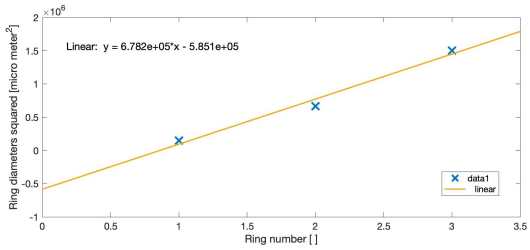

Fig. 21. Functional dependence of the squared diameters on the ring numbers

We obtain thus the slope γ and the intercept ϵ with the graph.

$$\gamma = \lambda/d = 6.782 \times 10^5\,\mu\text{m}^2 = 6.782 \times 10^{-7}\,\text{m}^2 \tag{33}$$

$$\epsilon = -5.851 \times 10^5\,\mu\text{m}^2 = -5.851 \times 10^{-7}\,\text{m}^2 \tag{34}$$

Equation (33) gives:

$$d = \frac{\lambda}{\gamma} = \frac{632.8 \times 10^{-9}}{6.782 \times 10{-}7} = 93.3\,\text{cm} \tag{35}$$

This value is about 10 times bigger than the actual distance between the mirrors. This error might be due to the fact that the picture of Figure 19 has low quality, and then the use of Figure 20 is not satisfying. Also, as indicated in the statement [1], a negative excess (i.e. $\epsilon < 0$) means an error in our analysis.
Let us see if an identification applied between Equations (36) and (37), can help for having better results.

$$D^2 = \frac{4f^2\lambda p}{d} + \frac{4f^2\lambda\epsilon}{d} \tag{36}$$

$$y = 6.782 \times 10^5 x - 5.851 \times 10^5 \tag{37}$$

where $f = 60\,\text{mm}$ the focal length of the focusing lens, $\lambda = 632.8\,\text{nm}$ is the wavelength of the light, $d = 12\,\text{cm}$ is the distance between the mirrors, p is the ring's number.

We have then Equation (38) in meters.

$$\frac{4f^2\lambda p}{d} = 6.782 \times 10^{-7}\,\text{m}^2 \tag{38}$$

$$(38) \Rightarrow d = \frac{4 \cdot 60 \cdot (10^{-3})^2 \cdot 632.8 \cdot 10^{-9}}{6.782 \cdot 10^{-7}} = 2.24 \times 10^{-4}\,\text{m}$$

It is clear that, here also, the distance between the mirrors is much to low (quarter of millimeter). Since the value of the sloped obtained by linear regression is used in identification for finding d, one can suppose that an error has been introduced in the analysis.
One can however determine the interference order m for this setup, in particular for $d = 12\,\text{cm}$, the effective distance between the mirrors that has been used during the laboratory session. It is given by Equation (39).

$$m = \frac{2d}{\lambda} = \frac{2 \cdot 12 \cdot 10^{-2}}{632.8 \cdot 10^{-9}} = 3.8 \times 10^5 \tag{39}$$

This allows us to deduce $\delta\nu$ the FSR, but also $\Delta\nu$ the full width at half maximum (FWHM).

$$\delta\nu = \frac{c}{2d} = \frac{3 \cdot 10^8}{2 \cdot 12 \cdot 10^{-2}} = 1.25\,\text{GHz} \tag{40}$$

$$\Delta\nu = \frac{\delta\nu}{F} = \frac{\delta\nu(1-R)}{\pi\sqrt{R}} \tag{41}$$

$$(41) \Rightarrow \Delta\nu = \frac{1.25 \cdot 10^9 \cdot (1 - 0.94)}{\pi \cdot \sqrt{0.94}} = 26.4\,\text{MHz}$$

These results are satisfying, they both belong to the normal range of such an interferometer [8].
Finally, the visibility for each peak can be computed to have an idea of how usable is the picture of Figure 19 to extract the data. A good visibility allows a good identification of the peak and thus good results. The visibility of a peak is defined in Equation (42) and has no dimension [1].

$$V(r) \equiv \frac{I_{max}(r) - I_{min}(r)}{I_{max}(r) + I_{min}(r)} \tag{42}$$

Table VI gives the results when we apply this formula on our data, where the intensities are given without dimension, relatively to a maximum of 255 and a minimum of 0, since these are coded in 8-bits.

TABLE VI
VISIBILITY OF THE PEAKS FOR ACCORDING TO THE RADIUS

Radius	I_{max}	I_{min}	Visibility
R_1	60	4	87%
R_2	54	12	64%
R_3	71	7	82%

VI. Final questions

Now that the experiments are well understood, the following problems are defined. They allow to get a good overview and a deeper understanding of the subject.

- Estimate the number of fays for an inteferometer with a finesse F. Compare your result using with the number N of lines for a typical grating, whose resolving power in the m^{th} order is given as $\frac{\lambda}{\Delta\lambda} = mN$. How do Fabry-Pérot resonators achieve their spectral resolution ?

There is a relation between the reflectivity of a lens and the notion of resolving power ($= \frac{\lambda}{\Delta\lambda}$) [7].

$$\frac{\lambda}{\Delta\lambda} = \frac{m\pi\sqrt{F}}{2} = \frac{m\pi R}{(1-R^2)} \tag{43}$$

This resolving power can also be defined as mN as explained in the statement. By equalizing both terms the relation (44) is obtained.

$$mN = \frac{m\pi R}{(1-R^2)} \iff N = \frac{\pi R}{(1-R^2)} \tag{44}$$

The higher the reflectivity, the higher the value of N so in order to achieve a high spectral resolution, the reflectivity needs to be as close to 100% as it can be.

- Give a reason why the free spectral range of a plane mirror cavity is always $\frac{c}{2d}$ whereas the FSR for confocal geometries may be just one half, i.e. $\frac{c}{4d}$ for pronounced off-axis beams. What is the FSR for concentric arrangements ($d = 2r$) ?

This point will explain why the value for the FSR in the experiments was set to $\frac{c}{4d}$. The development starts with the expression of the distance in terms of the wavelength. This will help defining the FSR as it is a measurement of the distance between two peaks.

$$d = \frac{n\lambda_1}{2}; d = \frac{(n+1)\lambda_2}{2} \tag{45}$$

Based on this observation, the differential of the wavelength can be written in the equation here under. This expression is valid because the two values are close.

$$\delta\lambda = \lambda_1 - \lambda_2 = \frac{2d}{n} - \frac{2d}{n+1} \tag{46}$$

$$(46) \implies \delta\lambda = \frac{2d}{n(n+1)} = \lambda_1\lambda_2$$

$$(46) \implies \frac{\delta\lambda}{\lambda_1\lambda_2} = 2d$$

For waves, $\nu = \frac{c}{\lambda}$ so we have $\delta\nu = \frac{c}{2d}$. In addition, as the cavity is a Fabry-Perot one, we have the path distance doubled so $\delta\nu = \frac{c}{4d}$. For concentric arrangements, we have $r_1 + r_2 = d$ so $\delta\nu = \frac{c}{2d}$.

- Calculate and plot the function $F_t(\rho)$ from Equation (47) for a mirror reflectivity of 96%. Why we don't use the beam expander for the confocal geometry ?

$$\frac{1}{F_t} = \sqrt{\left(\frac{1}{F_R}\right)^2 + \left(\frac{1}{F_q}\right)^2 + \left(\frac{1}{F_i}\right)^2} \tag{47}$$

In this equation, multiple terms can be found. The first one is F_R and represents the measured coefficient of the finesse previously found. The second term (F_q) is the mirror irregularities and will be considered infinite. The last term measures the influence of the displacement (ρ) on the total finesse according to Equation (48). This impact is plotted on Figure 22 for the two experiments (red for a $ROC = 75\ mm$ and green for a $ROC = 100\ mm$). Note that the limiting term is F_R.

$$F_i = \frac{ROC^3\lambda}{\rho^4} \tag{48}$$

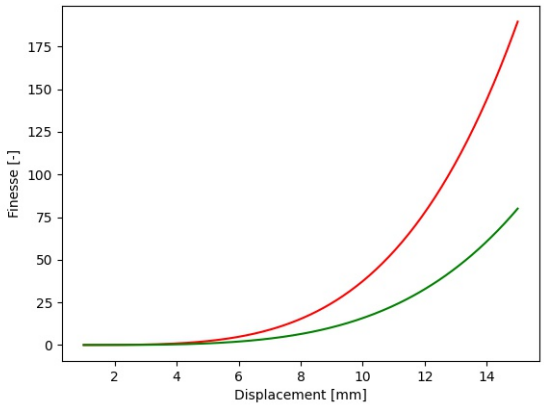

Fig. 22. $F_t(\rho)$: the evolution of the finesse with the displacement in the cavity

In a confocal geometry, a beam expander is not needed as their is no obligation to increase the probability of being reflected on a mirror with the good incidence angle to have a properly working system.

- Lasers often use spherical mirrors in the confocal distance ($d = r$). Why is this arrangement so important ?

For spherical mirrors, when we are in the configuration of the d distance between the mirrors equal to the ROC, we have Equation (49).

$$1 - \frac{d}{r_1} = 1 - \frac{d}{r_2} = 0 \tag{49}$$

In addition, the stability criterion for a resonator is given in Equation (50).

$$0 \leq \left(1 - \frac{d}{r_1}\right)\left(1 - \frac{d}{r_2}\right) \leq 1 \tag{50}$$

Then in this case, the criterion is equal to zero, which allows a good stability, robust to errors that can appear in the setup. (see Figure 17)

- An important feature of optical resonators is their "stability". Scan the literature and/or the web in order to find out how the criterion from Section 4.3 (statement) is derived – at least in principle. Is it a "yes/no" criterion or may the stability be quantified ?

Ray transfer matrix analysis [20] is used for translating the constraint for the system to be stable in a mathematical inequation: the stability criterion (see Inequation (50). In fact, the system is stable if and only if the beam stays in the cavity (and the spot size is a real and positive number). The cavity is unstable when the beam size grows until becoming bigger than the cavity. The consideration of stability is tangible as it depends on the cavity length. It can be quantified as the criterion product.

- The plane mirror mode gives reason for simple investigations of the mirror surface quality. Unlike spherical ones, imperfect plane mirrors cause serious wavefront errors after multiple back and forth reflections, since even tiny phase shifts induced by small deviations from the ideal plane surface add up and smear out the interference contrast. The surface roughness is often measured in fractions of the wavelength, $\Delta h = \frac{\lambda}{n}$. Values $\Delta h < \frac{\lambda}{100}$ cannot be realized without an extraordinary technical effort. As a consequence, the finesse is usually limited to $F = 50$, even for high reflecting mirrors. Figure 23 compares both limits. Give an explanation for the functional dependence on the right of Figure 23. Following this elementary theory, you can estimate the required surface quality of the mirrors used in our lab for an optimized finesse near the theoretical limit.

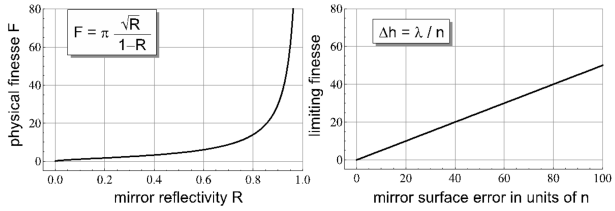

Fig. 23. The physical and technical finesse for plane mirrors. On the left, the reflection-based finesse F is shown. The technical limit is given in units of the wavelength fraction n (right) [1]

The finesse is linked to reflectivity and the surface quality of the mirrors. As the light makes back and forths in the cavity, if the a plane mirror has some defect in its confection, we can obtain some non-linearities due to the build-up of errors. The surface roughness is given by $\Delta = \frac{\lambda}{n}$ (where is n an integer and λ is the wavelength) with n often greater than 100.

The finesses computed in Sections III and IV are around 32 and 14. A good estimation of the required surface quality of the mirrors of the lab, for an optimized finesse can be deduced using Figure 23 (right side). The line drawn gives the relation between the limiting finesse and the mirror surface error in units of n. For a value of 32, the error is around 60 and for a finesse of 14 the error gets close to 18.

- Reconsider the concentric ring pattern in the plane mirror arrangement. Should the mirror distance d be enlarged or diminished in order to contract the ring diameters ?

The ring pattern appears because of back and forths of the light in the cavity, allowing diffraction. $\delta\nu$, the gap between two consecutive resoning frequencies (or FSR) is $\delta\nu = \frac{c}{2d}$. Then to get more contract ring diameters (i.e. small $\delta\nu$), we shall increase d.

- The visibility V describes the interference contrast. Find the functional dependence $V(F)$ on the finesse.

Optical laws give the visibility V related to the transmitted intensity T by Equation (51).

$$V = \frac{T_{max} - T_{min}}{T_{max} + T_{min}} \tag{51}$$

We also have Equation (52) linking T to the phase Φ of the light and to the finesse of the cavity.

$$T = \frac{1}{1 + (\frac{2}{\pi})^2 \cdot F^2 \cdot sin^2(\frac{\Delta\Phi}{2})} \tag{52}$$

From Equation (52), we obtain $T_{max} = 1$ for $\Delta\Phi \equiv 0[2\pi]$ and $T_{min} = \frac{1}{1+(\frac{2}{\pi})^2 \cdot F^2}$ for $\Delta\Phi \equiv \pi[2\pi]$.
From Equations (51) and (52), we obtain V, given by Equation (53).

$$V = \frac{(\frac{2}{\pi})^2 \cdot F^2}{2 + (\frac{2}{\pi})^2 \cdot F^2} \tag{53}$$

- Why did we use the polarizer and a CMOS camera for the plane-mirror experiment? Based on the measured wavelength distance for the two-mode spectrum, estimate if they could have been resolved by your plane-mirror setup. Reason your statement !

For the plane mirror experiment, a CMOS camera has been used to see the interference fringes. In this case, the polarizer was needed to split and differentiate two adjacent modes of the cavity.

VII. Conclusion

This laboratory was interesting because it made us improve two types of skills: practical and theoretical ones.

First, during the preparation, we had the opportunity to learn more about the theory behind the resonator. We understood, by analysing the formulas, the influences of each practical parameter on the propagating modes: the distance between the mirrors and their nature, the wavelength of the source, the mean... We also discovered some physical quantities to

characterize the interferometer, such as the finesse which gives the quality of the resonator [1], or also the free spectral range and the full width at half maximum which give information on the transmitted light. We now know which device to use with which parameters, if spectrometry has to be performed in later works.

In a practical manner, it is always satisfying for engineering students to touch and sense their object of study. This laboratory session with Tao, gave us the opportunity to have a good first appreciation of the construction and the use of such a device, including the calibration and the good alignment of the tools set. We had some difficulties at the beginning to observe the peaks on the oscilloscope in the first experiment, but after a while, all went good.

REFERENCES

[1] Michail Symeonidis, Toralf Scharf, Gabriele Pasquale, *Optics Laboratory Work: Fabry Perot Interferometer* [PDF]

[2] Wikipedia, *Helium–neon laser* [Internet]. https://en.wikipedia.org/wiki/Helium\OT1\textendashneon_laser

[3] Wikipedia, *Speed of light* [Internet]. https://en.wikipedia.org/wiki/Speed_of_light

[4] D. Briand, G. Villanueva, N. Quack, *Micro534 - Advanced MEMS @EPFL - Complement Slides Transduction* [PDF]

[5] Numephy, *Inteferences/coherence* [Internet]. http://res-nlp.univ-lemans.fr/NLP_C_M09_G01/co/Contenu_047.html

[6] Thorlabs, *CMOS CAMERAS: USB 2.0 AND USB 3.0* [PDF]. https://www.thorlabs.com/catalogpages/obsolete/2020/DCC1645C.pdf

[7] Unknown, *Lecture 19: Spectroscopy using Fabry-Perot interferometer* [Internet]. https://www.sheffield.ac.uk/polopoly_fs/1.171330!/file/PHY227-Lecture19_Spectroscopy.pdf

[8] RP Photonics, *Fabry–Pérot Interferometers* [Internet]. https://www.rp-photonics.com/fabry_perot_interferometers.html

[9] ATA scientific instruments, *Sprectrometry and spectroscopy: what's the difference?* [Internet]. https://www.atascientific.com.au/spectrometry/

[10] American Control Conference (ACC), *A tutorial on laser interferometry for precision measurements* [Conference paper]. https://www.researchgate.net/publication/261347353_A_tutorial_on_laser_interferometry_for_precision_measurements

[11] Optique pour l'ingénieur (OPI), *Mach-Zehnder Interferometer* [Internet]. http://www.optique-ingenieur.org/en/courses/OPI_ang_M02_C05/co/Contenu_24.html

[12] HyperPhysics, *Fabry-Perot Interferometer* [Internet]. http://hyperphysics.phy-astr.gsu.edu/hbase/phyopt/fabry.html

[13] RP Photonics, *Resonator Modes* [Internet]. https://www.rp-photonics.com/resonator_modes.html

[14] Edmund, *Laser resonator Modes* [Internet]. https://www.edmundoptics.com/knowledge-center/application-notes/lasers/laser-resonator-modes/

[15] Wikipedia, *Transverse mode* [Internet]. https://en.wikipedia.org/wiki/Transverse_mode

[16] Wikipedia, *Transverse mode* [Internet]. https://en.wikipedia.org/wiki/Transverse_mode

[17] Optique pour l'ingénieur (OPI), *Longitudinal and transverse modes* [Internet]. http://www.optique-ingenieur.org/en/courses/OPI_ang_M01_C03/co/Contenu_02.html

[18] eLas GmbH, Eschbach (2009) *Laser Education Kit – CA-1140 Fabry Perot Resonator* [User Manual].

[19] B.E.A. Saleh and M.C. Teich (2013) *Fundamentals of photonics* [Book].

[20] Allan Gillespie - Carnegie Laboratory of Physics University of Dundee - Scotland (2013) *Comparison between charged-particle (CP) and light/laser (L) optics* [Internet]. https://indico.cern.ch/event/266133/attachments/474621/656940/Gillespie_Aachen_CP_vs_P_optics.pdf

VIII. APPENDIX

A. Different machines and software

Three experiments were performed during the laboratory and different measurements machines were used. To avoid repetition, all the machines are presented in this section and will be refereed to in the texts in the following sections.

1) HeNe laser: The laser used is a Helium Neon based laser with a behaviour as described in the theoretical background. The maximal output power is $5\ mW$ with a wavelength of $632.8\ nm$. This laser is part of the class $3B$ and therefore glasses have been worn during the laboratory. This laser has to orthogonal polarizations. This last specification will be important for Section V

2) Piezo ceramic actuator: The type of piezo ceramic actuator used is $HPSt500/15-8/7$. It has a maximal output voltage of $150\ V$ and a open loop sensitivity of approximately $0.05\ nm$ for $5\ mV$. The force produce by the device can go up to $5500\ N$. The maximal stroke is $13/8\ \mu m$, the length is $26\ mm$, the capacitance is $140\ nF$, the stiffness is $550\ N/\mu m$ and the resonance of $30\ kHz$.

3) Photo diode: The photo diode is a camera from Siemens (Siemens BPX 61). It has a photodetector of area $2.65\ mm \times 2.65\ mm$ which allows to collect even the unfocused light with $FMWH$ higher than $1\ mm$ without losing too much information. The camera works for a range of wavelengths between $400\ nm$ and $1100\ nm$ with an optimal operating point of $850\ nm$. The working wavelength being under the optimal value it won't cause important degradation in the performances as explained in Section II

Fig. 24. Photo diode (Siemens BPX 61)

4) Control unit: The tool used to control the piezo ceramic actuator is a $PTC1000$ control unit (right part on Figure 25). It can control the piezo in terms of frequency, amplitude and offset and the voltage profile created can be triangular or saw tooth. This control unit is also responsible for the processing of the photo diode output signal (left part on Figure 25).

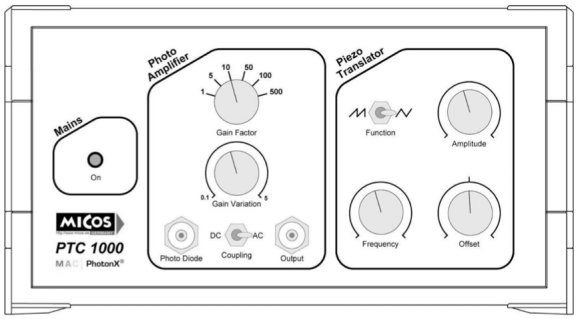

Fig. 25. Front panel of the control unit PTC 1000. In the "photo amplifier" unit, the gain may be varied within 0.1 and 2500. The frequency of the piezo triangle (or saw tooth) voltage can be set between 50 Hz and 100 Hz

5) Oscilloscope: The oscilloscope used in this laboratory is a Rohde Schwarz $HMO2024$ with a bandwidth of 200 MHz. It is connected to the control unit allowing the visualization of the signals coming from it. This device has 3 channels where the first one will show the output of the photo diode and the second one will show the piezo triangle voltage. The screen shots in this laboratory are directly exported from the oscilloscope.

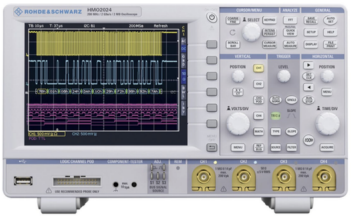

Fig. 26. Front panel of the HMO2024. An additional USB port for connection with a PC (remote control) is located on the back of the instrument.

6) CMOS camera DCC1545M [6]: This camer can be plugged to a computer by a USB 2.0 cable. Its resolution is 1280 x 1024 pix square, for a pixel size of $5.2\,\mu m$. Its sensor is monochromatic which explains why the images we obtain are black and white, even if the laser emits red light.

Fig. 27. DCC1545M Thorlabs CMOS camera

7) ThorCam™ Software: This software allow image acquisition is designed for use with our cameras for Scientific and Compact USB Cameras

B. Script

```
diameters = [383, 815, 1226]
numb_ring = [1, 2, 3]

plot (numb_ring,diameters.*diameters,'x')
title('Functional dependence of the
    squared diameters on the ring number')
ylabel('Ring diameters squared
    [micro meter^2]');
xlabel('Ring number [ ]');
```

Fig. 28. Matlab code for plotting the ring diameters on the rings number